Development/Plasticity/Repair

Repetitive Magnetic Stimulation Induces Functional and Structural Plasticity of Excitatory Postsynapses in Mouse Organotypic Hippocampal Slice Cultures

Andreas Vlachos,[1]* Florian Müller-Dahlhaus,[1,2]* Johannes Rosskopp,[1,2] Maximilian Lenz,[1] Ulf Ziemann,[2,3]† and Thomas Deller[1]†

[1]Institute of Clinical Neuroanatomy, Neuroscience Center, and [2]Department of Neurology, Goethe-University Frankfurt, D-60590 Frankfurt/Main, Germany, and [3]Department of Neurology and Stroke, Hertie Institute for Clinical Brain Research, Eberhard-Karls-University Tübingen, D-72076 Tübingen, Germany

Repetitive transcranial magnetic stimulation (rTMS) is a noninvasive brain stimulation technique that can alter cortical excitability in human subjects for hours beyond the stimulation period. It thus has potential as a therapeutic tool in neuropsychiatric disorders associated with alterations in cortical excitability. However, rTMS-induced neural plasticity remains insufficiently understood at the cellular level. To learn more about the effects of repetitive magnetic stimulation (rMS), we established an *in vitro* model of rMS using mouse organotypic entorhino-hippocampal slice cultures. We assessed the outcome of a high-frequency (10 Hz) rMS protocol on functional and structural properties of excitatory synapses in mature hippocampal CA1 pyramidal neurons. Whole-cell patch-clamp recordings, immunohistochemistry, and time-lapse imaging techniques revealed that rMS induces a long-lasting increase in glutamatergic synaptic strength, which is accompanied by structural remodeling of dendritic spines. The effects of rMS on spine size were predominantly seen in small spines, suggesting differential effects of rMS on subpopulations of spines. Furthermore, our data indicate that rMS-induced postsynaptic changes depend on the NMDA receptor-mediated accumulation of GluA1-containing AMPA receptors. These results provide first experimental evidence that rMS induces coordinated functional and structural plasticity of excitatory postsynapses, which is consistent with a long-term potentiation of synaptic transmission.

Introduction

Repetitive transcranial magnetic stimulation (rTMS) is a safe and painless noninvasive brain stimulation technique that has recently received increasing interest as a therapeutic neurorehabilitative tool (Hallett, 2007). It is now well established that high-frequency rTMS (several hundred pulses at frequencies ≥5 Hz) increases human cortical excitability for minutes and even hours beyond the stimulation period (for review, see Ziemann et al., 2008). In the motor cortex, these aftereffects of rTMS can be measured by the size of the electromyographic response that is evoked by a single standard suprathreshold TMS pulse in the target muscle. In nonmotor areas, long-lasting rTMS effects were demonstrated based on neuroimaging techniques (for review, see Siebner et al., 2009) and EEG recordings (Thut and Pascual-Leone, 2010). These aftereffects have been proposed to represent long-lasting changes of synaptic efficacy (Thickbroom, 2007) and were therefore termed "long-term potentiation (LTP)-like" phenomena. However, whether rTMS indeed affects synaptic strength at the single-cell level has not yet been conclusively demonstrated.

A set of studies has started addressing the cellular mechanisms underlying rTMS-induced plasticity (Levkovitz et al., 1999; Keck et al., 2001; Moliadze et al., 2003; Valero-Cabré et al., 2005; Ahmed and Wieraszko, 2006; Trippe et al., 2009; Benali et al., 2011; Gersner et al., 2011; Salinas et al., 2011; Hellmann et al., 2012). It is clear that studies using animal models or appropriate *in vitro* preparations are urgently needed to unravel the effects of rTMS on neural plasticity. Data from such studies could guide the development of successful therapeutic strategies using noninvasive brain stimulation techniques (Ridding and Rothwell, 2007). Therefore, in the present study, we have established an *in vitro* model of repetitive magnetic stimulation (rMS) using mouse entorhino-hippocampal slice cultures (Stoppini et al., 1991; Frotscher et al., 1995; Gähwiler et al., 1997). In these organotypic cultures, neuronal connectivity is well preserved, allowing rMS experiments to be performed in a standardized and highly reproducible manner similar to *in situ* conditions. In addition, neurons in these cultures are readily accessible for functional as well as structural analyses.

Received Jan. 26, 2012; revised Sept. 21, 2012; accepted Oct. 21, 2012.

Author contributions: A.V., F.M.-D., U.Z., and T.D. designed research; A.V., F.M.-D., J.R., and M.L. performed research; A.V., F.M.-D., J.R., and M.L. analyzed data; A.V., F.M.-D., U.Z., and T.D. wrote the paper.

The work was supported by funding from the Heinrich und Erna Schaufler-Stiftung (A.V., F.M.-D., U.Z., T.D.), the Medical Faculty of Goethe University Frankfurt (F.M.-D.), and the Interdisciplinary Center for Neuroscience Frankfurt (A.V., F.M.-D., U.Z., T.D.). We thank Charlotte Nolte-Uhl and Nadine Zahn for skillful assistance in tissue culturing.

The authors declare no competing financial interests.

*A.V. and F.M.-D. contributed equally to this work.

†U.Z. and T.D. contributed equally to this work.

Correspondence should be addressed to either Andreas Vlachos or Florian Müller-Dahlhaus, Theodor-Stern Kai 7, Goethe-University, 60590 Frankfurt am Main, Germany. E-mail: a.vlachos@med.uni-frankfurt.de or f.mueller@med.uni-frankfurt.de.

DOI:10.1523/JNEUROSCI.0409-12.2012

 0270-6474/12/3217514-10$15.00/0

To validate this *in vitro* approach and to learn more about the cellular effects of rMS, we have assessed the capability of rMS to induce functional and structural plasticity of excitatory hippocampal synapses. We report that high-frequency (10 Hz) rMS has a long-lasting effect on glutamatergic synaptic strength of CA1 pyramidal neurons, which is accompanied by postsynaptic structural plasticity at the level of individual dendritic spines. Of note, the effect of rMS on spine morphology was predominantly seen in small spines, suggesting that rMS can have distinct effects on subpopulations of spines. Furthermore, our data indicate that rMS interferes with the postsynaptic accumulation of GluA1-containing AMPA receptors (AMPA-Rs), which critically depends on the activation of NMDA receptors (NMDA-Rs) during rMS. Thus, we provide, to the best of our knowledge, first evidence for rMS-induced changes in functional and structural properties of excitatory postsynapses at the cellular level.

Materials and Methods

Preparation of slice cultures. Experimental procedures were performed in agreement with the German law on the use of laboratory animals and approved by the animal welfare officer of Goethe-University Frankfurt, Faculty of Medicine. Entorhino-hippocampal slice cultures were prepared at postnatal day 4–5 from C57BL/6J×BALB/cJ or Thy1-GFP mice (Feng et al., 2000) of either sex as previously described (Vlachos et al., 2012a). Cultivation medium contained 50% (v/v) MEM, 25% (v/v) Basal Medium Eagle, 25% (v/v) heat-inactivated normal horse serum, 25 mM HEPES buffer solution, 0.15% (w/v) bicarbonate, 0.65% (w/v) glucose, 0.1 mg/ml streptomycin, 100 U/ml penicillin, and 2 mM glutamax. The pH was adjusted to 7.3, and the medium was replaced every second day. All slice cultures were allowed to mature for at least 18 d in humidified atmosphere with 5% CO_2 at 35°C.

Repetitive magnetic stimulation. For rMS, 3- to 4-week-old cultures [18–30 d *in vitro* (div)] were transferred to a 30 mm Petri dish containing warm (~35°C) standard extracellular solution (129 mM NaCl, 4 mM KCl, 1 mM $MgCl_2$, 2 mM $CaCl_2$, 4.2 mM glucose, 10 mM HEPES, 0.1 mg/ml streptomycin, 100 U/ml penicillin, pH 7.4 with KOH; osmolarity was adjusted with sucrose to match cultivation medium). Cultures were stimulated using a Magstim Rapid magnetic stimulator with two booster modules (Magstim Company) connected to a standard 70 mm outer wing diameter double coil (Magstim Company). Cultures were placed ~1 cm below the center of the coil (i.e., junction of the two wings) (Fig. 1*A*) and stimulated with a high-frequency stimulation protocol consisting of nine trains of 100 pulses each at 10 Hz with an intertrain interval of 30 s. Regular rTMS protocols at a fixed frequency of 5–20 Hz have been shown to induce facilitatory aftereffects in most studies reported in the literature (for review, see Ziemann et al., 2008; Thut and Pascual-Leone, 2010). Orientation of cultures was such that the induced electric field within the tissue was approximately orthogonal to the Schaffer collaterals, the main afferent input to hippocampal CA1 pyramidal neurons (Fig. 1*B*). Stimulation intensity was set to 50% of maximum stimulator output. In some experiments, D-APV (50 μM) was used to block NMDA-Rs during stimulation. After magnetic stimulation, cultures were transferred back to the incubator for at least 20 min before experimental assessment. Control cultures were not stimulated, but otherwise treated identical to stimulated cultures (age- and time-matched controls).

Whole-cell patch-clamp recordings. Whole-cell voltage-clamp recordings from CA1 pyramidal neurons (up to five neurons per culture) were performed at 35°C (for details, see Vlachos et al., 2012b). The bath solution contained 126 mM NaCl, 2.5 mM KCl, 26 mM $NaHCO_3$, 1.25 mM NaH_2PO_4, 2 mM $CaCl_2$, 2 mM $MgCl_2$, and 10 mM glucose. Patch pipettes contained 126 mM K-gluconate, 4 mM KCl, 4 mM ATP-Mg, 0.3 mM GTP-Na_2, 10 mM PO-creatine, 10 mM HEPES, and 0.3% biocytin (pH 7.25 with KOH, 290 mOsm with sucrose) having a tip resistance of 6–10 MΩ. In some experiments, Alexa 488 or Alexa 568 (10 μM) was added to the internal solutions for visualization of neuronal morphology before recordings. Neurons were recorded at −70 mV in the presence of 10 μM D-APV, 10 μM 4-[6-imino-3-(4-methoxyphenyl)pyridazin-1-yl]butanoic acid hydrobromide (SR-95531), and 0.5 μM TTX. For recordings of NMDA-R-mediated miniature EPSCs (mEPSCs) at +40 mV, the internal solution contained 117 mM $CsCH_3SO_3$, 20 mM HEPES, 0.4 mM EGTA, 5 mM TEA, 5 mM QX314, 4 mM ATP-Mg, and 0.3 mM GTP-Na_2. Neurons were recorded in the presence of 10 μM CNQX, 10 μM SR-95531, and 0.5 μM TTX in these experiments. Series resistance was monitored in 2 min intervals, and recordings were discarded if the series resistance and leak current changed significantly and/or reached ≥30 MΩ or ≥150 pA, respectively. Recordings from control (baseline) and stimulated cultures [0–2, 2–4, 4–6, and 6–8 h post-magnetic stimulation (pms); 2–4 h after stimulation in D-APV] were obtained in pseudo-randomized order to avoid any acquisition bias.

Immunostaining and imaging. Cultures were fixed in a solution of 4% (w/v) paraformaldehyde (PFA) in PBS (0.1 M, pH 7.4) and 4% (w/v) sucrose for 1 h, followed by 2% PFA and 30% sucrose in PBS overnight. Cryostat sections (40 μm) of fixed slice cultures were prepared and stained with antibodies against synaptophysin or GluA1 following a protocol previously described (Vlachos et al., 2008, 2009). Briefly, sections were incubated for 1 h with 10% normal goat serum in 0.1% Triton X-100 containing PBS to reduce unspecific staining and subsequently incubated for 24 h at 4°C in mouse anti-synaptophysin antibody (Millipore; MAB 5258) or rabbit anti-GluA1 antibody (Millipore; AB 1504). Sections were washed and incubated for 1 h with Alexa 488- and 568-labeled goat anti-mouse and anti-rabbit antibody, respectively (Invitrogen; 1:1000; 10% normal goat serum, 0.1% Triton X-100). F-actin was stained with Alexa 488- or 568-labeled phalloidin (Invitrogen; 1:100; 45 min). TO-PRO (Invitrogen) nuclear stain was used to visualize culture cytoarchitecture (1:30,000; 10 min). Sections were washed again, transferred onto glass slides, and mounted for visualization with antifading mounting medium. Confocal images were acquired using a Nikon Eclipse C1si laser-scanning microscope with a 10× [numerical aperture (NA), 0.30; Nikon] and a 60× oil-immersion (NA 1.3; Nikon; 8× scan zoom) objective lens, respectively. Detector gain and amplifier were initially set to obtain pixel densities within a linear range. All images were sampled with ideal Nyquist rate.

Time-lapse imaging of slice cultures. Live imaging of slice cultures was performed as previously described (Vlachos et al., 2012a) in standard extracellular solution (for details, see above, Repetitive magnetic stimulation) and additionally containing 0.1 mM Trolox (Sigma-Aldrich). Cultures were imaged with an upright Zeiss LSM Pascal confocal microscope. Dendritic segments in the stratum radiatum from side branches of the apical dendrites of hippocampal CA1 pyramidal neurons were visualized with a 63× objective lens (0.95 NA; Zeiss). Image stacks were captured at 4× scan zoom with ideal Nyquist rate. Up to 25 images were recorded per stack. Per culture, only one to two segments were visualized to minimize dwell time during imaging procedure (<10 min per culture) and phototoxic damage.

Quantification and statistics. Electrophysiological data were analyzed using pClamp 10.2 (Molecular Devices) and MiniAnalysis (Synaptosoft) software. All events were visually inspected and detected by an independent investigator blind to experimental condition. One hundred fifty to 350 events were analyzed per recorded neuron in the mEPSC experiments. Statistical comparisons were made using a factorial ANOVA to test for the effect of TIME in the AMPA-R mEPSC time course analysis (five levels: baseline, 0–2, 2–4, 4–6, and 6–8 h pms). Unpaired *t* tests were used to compare mEPSC recordings in the D-APV experiments. Age- and time-matched controls were pooled, since no statistical significance was observed between control groups. The Wilcoxon–Mann–Whitney test was used to compare electrophysiological data obtained in the NMDA-mEPSCs and paired recordings experiments.

Mean fluorescence intensity of synaptophysin, F-actin, and GluA1 stainings, and size/number of immunolabeled GluA1 clusters were determined in CA1 stratum radiatum using the ImageJ software package (available from http://rsb.info.nih.gov/ij) as previously described (Bas Orth et al., 2005). Statistical comparisons were made using the Wilcoxon signed rank sum test (optical density analysis) and the Wilcoxon–Mann–Whitney test (D-APV GluA1 cluster analysis). A factorial ANOVA was

used to test for the effect of TIME in the GluA1 cluster time course analysis (six levels: control and 1, 2, 3, 4, and 6 h pms).

Dendritic spines were assessed manually on 3D image stacks of independent dendritic segments using the Zeiss LSM image browser (Vlachos et al., 2012a). All dendritic protrusions were counted as dendritic spines, regardless of their morphological characteristics. Images were analyzed blind to experimental condition to ensure unbiased observation. For each segment, a defined distance (~30 μm) from an identified branch point was analyzed and spine densities were calculated. Maximal cross-sectional areas of individual spines were determined in confocal image stacks as previously described (Vlachos et al., 2009). Spines were categorized into three approximately equal subclasses by size: small spines, maximal cross-sectional area [x] $< 0.45\ \mu m^2$; medium spines, $0.45\ \mu m^2 \leq x < 0.65\ \mu m^2$; and large spines, $x \geq 0.65\ \mu m^2$, respectively. Spine sizes in these subgroups were not different between control and rMS groups before treatment ($p > 0.2$ for each comparison, unpaired t test). Data from time points 2, 3, 4, and 6 h after treatment were normalized to those from 0 h (before treatment) and averaged per individual dendritic segment. In addition, changes in spine size in the rMS group were corrected for spontaneous fluctuations in mean spine size (Yasumatsu et al., 2008) of the respective spine subgroups in the control group. Statistical comparisons for changes in spine density and size were made using repeated-measures ANOVA to test the within-group effect of TIME (five levels: 0, 2, 3, 4, 6 h after rMS) and the between-group effect of TREATMENT (two levels: control, rMS). Unpaired t tests were used to compare spine size data in the D-APV experiments (age- and time-matched control data pooled with control data shown in Fig. 3 since no statistical significance was observed between control groups).

In all ANOVAs, *post hoc* testing was performed using t tests to examine differences between the single levels of significant main effects or their interactions. Values of $p < 0.05$ were considered a significant difference. All values are expressed as mean ± SEM.

Digital illustrations. Confocal image stacks were exported as 2D projections and stored as TIFF files. Figures were prepared using Photoshop graphics software (Adobe). Image brightness and contrast were adjusted.

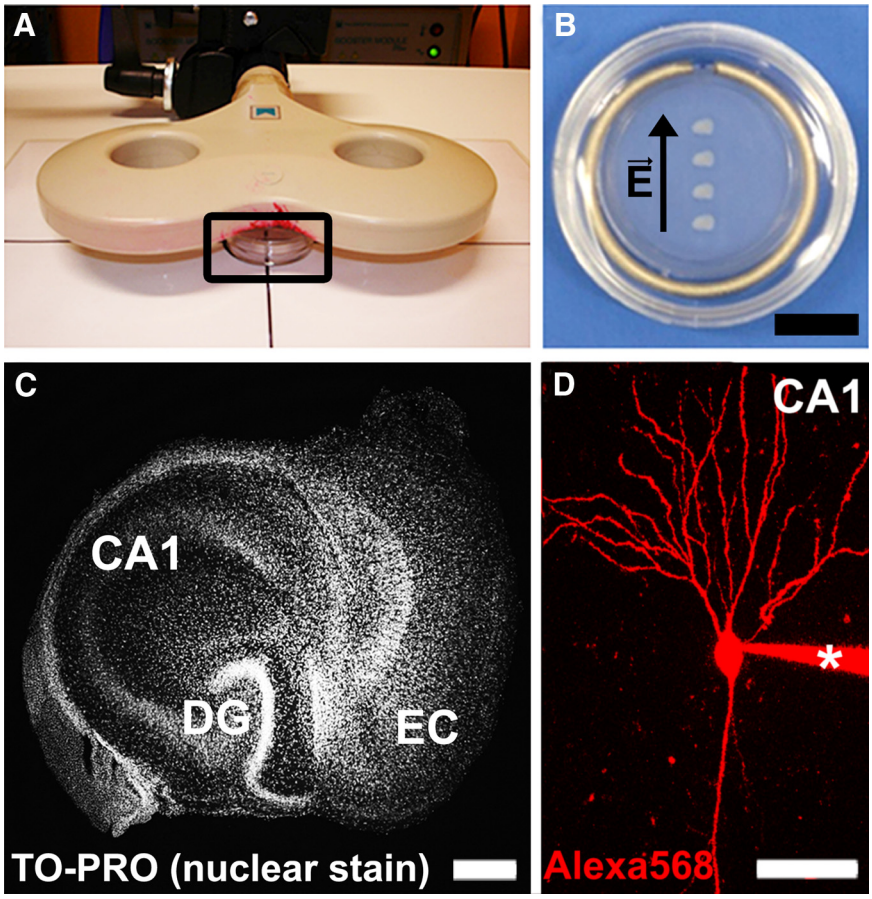

Figure 1. Repetitive magnetic stimulation of mouse entorhino-hippocampal slice cultures. ***A***, Slice cultures were stimulated with a standard 70 mm outer wing diameter figure-of-eight double coil (Magstim Company). Distance from coil, position and orientation of cultures (boxed area) within the magnetic field were kept constant in all experiments. ***B***, Orientation of slice cultures. All cultures were placed in parallel so that entorhinal cortex and hippocampus were orientated in the same direction. Thus, the induced electric field within the tissue ($\vec{E}$; arrow) was approximately orthogonal to the Schaffer collaterals, the main afferent input to hippocampal CA1 pyramidal neurons. Four to five cultures were stimulated at the same time. Scale bar, 5 mm. ***C***, Entorhino-hippocampal slice culture stained with TO-PRO nuclear stain at high magnification. Orientation of slice cultures as in ***B***. Effects of rMS were studied in area CA1 (DG, dentate gyrus; EC, entorhinal cortex). Scale bar, 150 μm. ***D***, CA1 pyramidal neuron with attached patch-clamp pipette (asterisk) filled with Alexa 568. Scale bar, 50 μm.

Results

Repetitive magnetic stimulation induces changes of excitatory synaptic strength

To assess rMS-induced changes in excitatory synaptic strength individual CA1 pyramidal neurons of mature (≥18 div) entorhino-hippocampal slice cultures were patched (Fig. 1*C*,*D*) and mEPSCs were recorded in whole-cell voltage-clamp mode under control conditions (age- and time-matched nonstimulated but otherwise equally treated cultures) and between 0 and 2 h, 2 and 4 h, 4 and 6 h, and 6 and 8 h pms (Fig. 2). Recordings were performed at a holding potential of −70 mV in the presence of TTX (0.5 μM), which inhibits sodium channels and blocks network activity, as well as inhibitors of NMDA-Rs (D-APV; 10 μM) and $GABA_A$ receptors (SR-95531; 10 μM). Accordingly, we were able to assess properties of AMPA-R-mediated inward currents evoked by stochastic release of glutamate from presynaptic terminals (Fig. 2*A*), which could be blocked by the AMPA-R inhibitor CNQX (10 μM). Although various conditions may account for the results obtained by mEPSC recordings [discussed by Lisman (2009)], the amplitude of these quantal events is considered to reflect postsynaptic strength, whereas the frequency of mEPSCs represents either presynaptic properties (e.g., changes in vesicle pool size/release probability) or changes in the total number of active synapses. Our whole-cell recordings revealed that rMS leads to a significant increase in mEPSC amplitude ($F_{(4,92)} = 7.74$; $p < 0.0001$) and frequency ($F_{(4,92)} = 9.38$; $p < 0.0001$) compared with nonstimulated and otherwise equally treated control cultures (Fig. 2*B–D*). While the frequency was increased at all time points pms (Fig. 2*D*), a significant increase in mEPSC amplitude was detected between 2 and 6 h pms only (Fig. 2*C*). At 6–8 h pms, the mEPSC amplitudes returned back to baseline. We concluded from these experiments that rMS induces long-lasting changes in AMPA-R-mediated glutamatergic neurotransmission of cultured CA1 pyramidal neurons.

Postsynaptic structural changes accompany rMS-induced changes in mEPSCs

We next evaluated whether rMS also induced structural changes that could be related to the observed functional changes (Fig. 3).

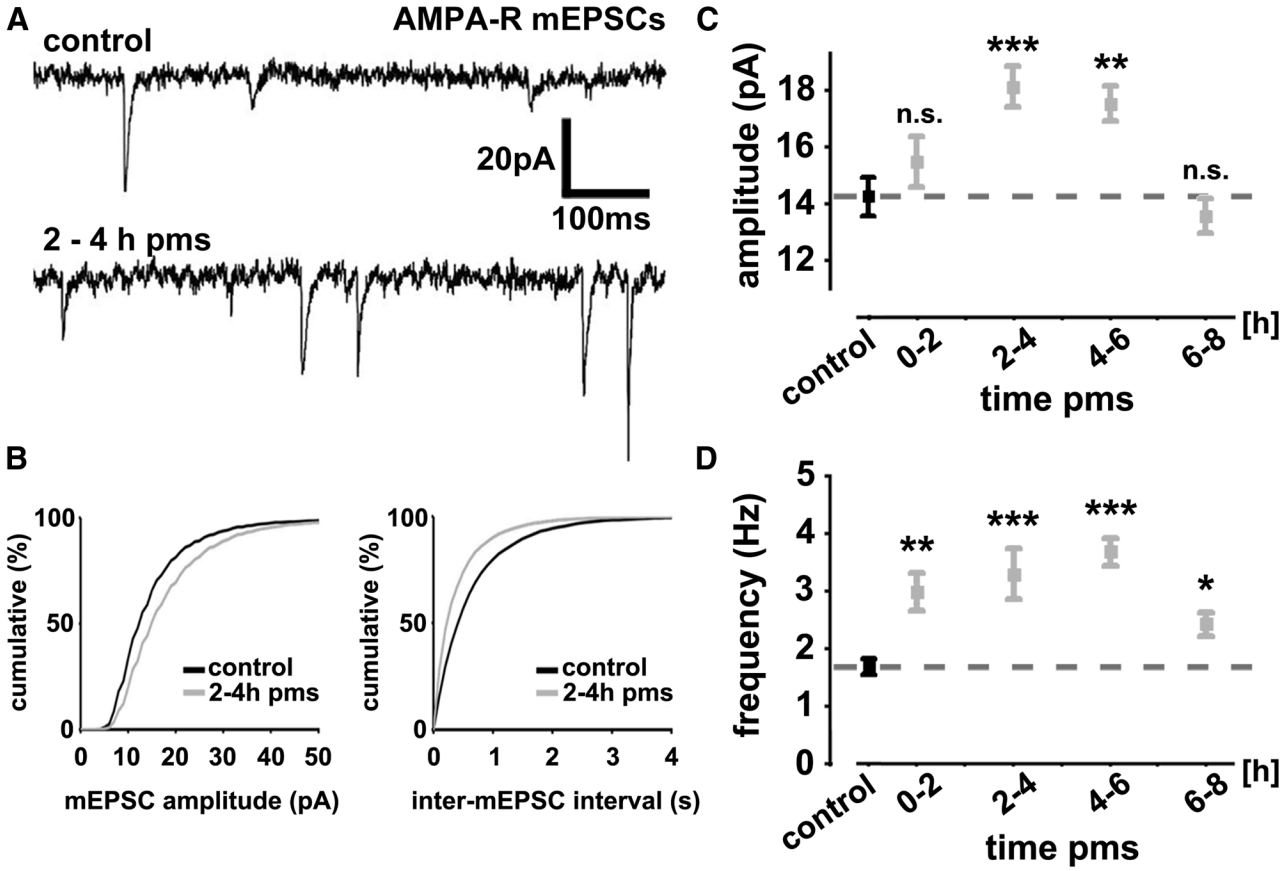

Figure 2. Repetitive magnetic stimulation induces a long-lasting increase in excitatory synaptic transmission *in vitro*. ***A***, Sample traces of AMPA-R-mediated mEPSCs from control and stimulated hippocampal CA1 pyramidal neurons. ***B***, Cumulative distributions of AMPA-R-mediated mEPSC amplitudes and inter-mEPSC intervals. ***C***, ***D***, A significant increase in mean mEPSC amplitudes (***C***) was observed between 2 and 6 h pms, while mEPSC frequencies (***D***) were found to be increased at all time points recorded after magnetic stimulation ($n = 14–27$ neurons per group, with up to 5 recorded neurons per culture and 5–11 cultures per group; 97 neurons total). Statistical comparisons were performed with pooled nonstimulated age- and time-matched controls (indicated by dashed line). Means ± SEM are shown in this and the following figures ($*p < 0.05$; $**p < 0.01$; $***p < 0.001$).

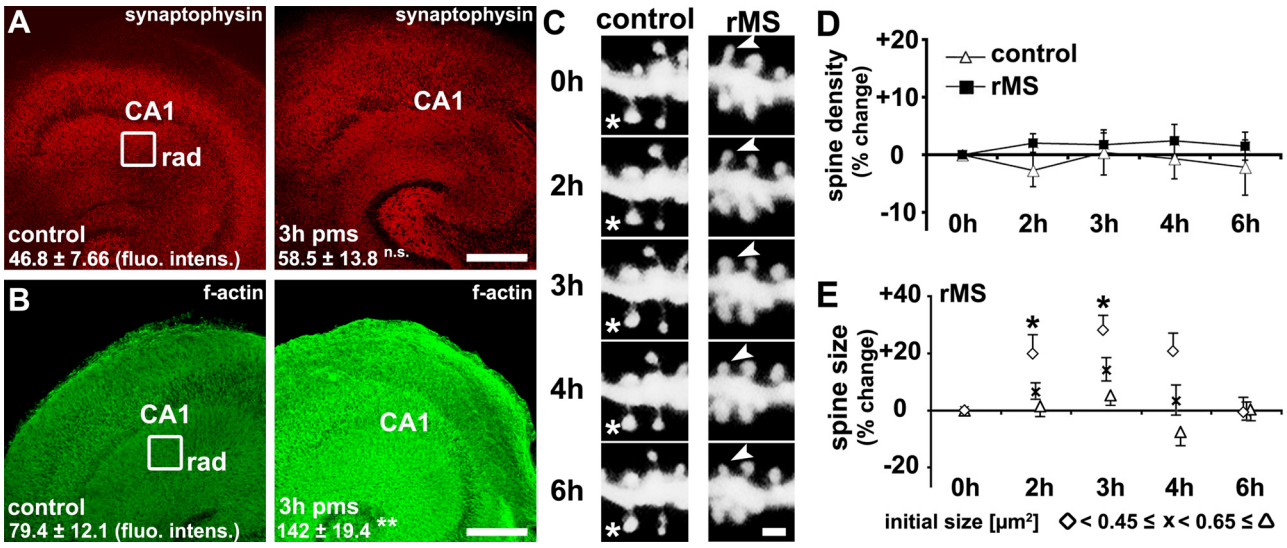

Figure 3. Repetitive magnetic stimulation *in vitro* induces postsynaptic structural plasticity in CA1 stratum radiatum. ***A***, ***B***, Samples of nonstimulated age- and time-matched control (left column) and stimulated (right column) slice cultures fixed at 3 h pms stained for synaptophysin (***A***; $n = 6$) and F-actin (***B***; $n = 11$). The mean fluorescence intensity was analyzed in the stratum radiatum (rad) of area CA1. A significant increase in F-actin, but not in synaptophysin fluorescence intensity (fluo. intens.) was observed. Scale bar, 150 μm. ***C–E***, Time-lapse imaging of identified individual spines of side branches of apical dendrites of GFP-expressing CA1 pyramidal neurons in the stratum radiatum (***C***) revealed no significant changes in spine density (***D***), but changes in spine size following rMS (***E***; $n = 10$ control vs $n = 13$ rMS segments; from 10 control and 13 rMS-treated cultures, respectively). Spines with a small initial size demonstrated a significant increase in size following rMS (***E***). Note that data presented in ***E*** demonstrate spine sizes from identified individual spines repeatedly measured pms at given time points, corrected for spontaneous fluctuations in mean spine size of the respective spine groups (small, $<0.45\ \mu m^2$; medium, $0.45\ \mu m^2 \leq x < 0.65\ \mu m^2$; large, $\geq 0.65\ \mu m^2$) in the control group. The asterisks in ***C*** indicate a spine in control cultures that does not change in size; the arrowheads point at a small spine that transiently increases in size after rMS. Scale bar: ***C***, 1 μm.

Stimulated and nonstimulated slice cultures were fixed at 3 h pms and stained for the presynaptic marker synaptophysin (Fig. 3*A*), as well as for F-actin (Fig. 3*B*), which served as a postsynaptic marker in this set of experiments. While the mean synaptophysin immunofluorescence in the stratum radiatum of area CA1 was not affected at 3 h pms ($p = 0.46$), we detected a significant increase in mean fluorescence intensity of F-actin in stimulated cultures ($p = 0.008$). Although these results did not exclude the possibility of presynaptic changes in response to rMS, they prompted us to look for rMS-induced structural changes of excitatory postsynapses.

Repetitive magnetic stimulation induces dendritic spine plasticity

Since most excitatory postsynapses form on actin-rich dendritic spines in cortical neurons (Harris et al., 1992; Takumi et al., 1999a,b; Capani et al., 2001), and synaptic plasticity is accompanied by structural changes of spines (Engert and Bonhoeffer, 1999; Maletic-Savatic et al., 1999; Fukazawa et al., 2003; Jourdain et al., 2003; Segal et al., 2003; Matsuzaki et al., 2004; Nägerl et al., 2004), we next assessed the effects of rMS on spine remodeling. A time-lapse imaging approach was used in this set of experiments (Vlachos et al., 2012a). Imaging of the same identified side branches of apical dendrites of GFP-expressing CA1 pyramidal neurons in the stratum radiatum was performed before (0 h) and at 2, 3, 4, and 6 h pms (Fig. 3*C–E*).

First, spine densities were determined, as a higher number of spine synapses could account for the observed increase in F-actin fluorescence and mEPSC frequency after rMS. No significant changes in spine density were detected between the two groups in these experiments ($F_{(1,21)} = 0.74$, $p = 0.40$ for TREATMENT; Fig. 3*D*). Both, stimulated and nonstimulated cultures demonstrated a constant spine density throughout the observation period ($F_{(4,84)} = 0.27$, $p > 0.5$ for TIME; $F_{(4,84)} = 0.51$, $p > 0.5$ for the interaction TREATMENT with TIME). We concluded that spine densities of side branches of apical dendrites of CA1 pyramidal neurons in the stratum radiatum are not altered by rMS in our experimental conditions.

Evidence exists that links the strength of excitatory postsynapses to spine geometry: weak AMPA-R-mediated postsynaptic currents are associated with small spines, whereas strong currents can be elicited preferentially in large spines (Matsuzaki et al., 2001; Harvey and Svoboda, 2007; Holbro et al., 2009; Vlachos et al., 2009). We, therefore, assessed relative changes in maximal cross-sectional areas of the same individual spines [identified at 0 h (i.e., before rMS)] at 2 h, 3 h, 4 h and 6 h pms. Indeed, these experiments showed that rMS increases mean spine size with respect to nonstimulated control cultures (2 h pms: $+9.8 \pm 4.3\%$; 3 h pms: $+17.7 \pm 4.0\%$; 4 h pms: $+9.1 \pm 3.6\%$; 6 h pms: $+3.2 \pm 4.2\%$; $F_{(1,21)} = 6.31$, $p = 0.02$ for TREATMENT; $F_{(4,84)} = 2.52$, $p = 0.047$ for the interaction TREATMENT with TIME; data corrected for spontaneous fluctuations in mean spine size of the control group). *Post hoc* testing revealed that mean spine size was significantly increased at 3 h pms ($p = 0.0056$) with a trend toward spine size increases at 2 h ($p = 0.09$) and 4 h ($p = 0.097$) pms, but was not significantly different between stimulated and nonstimulated cultures at 6 h pms ($p > 0.5$). Thus, rMS of entorhino-hippocampal slice cultures leads to the enlargement of dendritic spines of CA1 pyramidal neurons in stratum radiatum.

As spines of different size and morphology may serve different functional roles (Matsuzaki et al., 2004), we categorized spines into three equal subgroups according to their initial size (small spines, initial maximum cross-sectional area [x] $< 0.45\ \mu m^2$; mean spine size: $0.31 \pm 0.005\ \mu m^2$; medium spines, $0.45\ \mu m^2 \leq x < 0.65\ \mu m^2$; mean spine size: $0.54 \pm 0.004\ \mu m^2$; large spines, $x \geq 0.65\ \mu m^2$; mean spine size: $0.90 \pm 0.018\ \mu m^2$; Fig. 3*E*). Separate repeated-measures ANOVAs for the three spine subgroups showed that in particular small spines increased in size over time, with a maximum increase in cross-sectional area of ~30% at 3 h pms (Fig. 3*E*; effect of TIME: $F_{(4,84)} = 4.46$, $p = 0.0026$). There was a significant effect of the interaction TIME with TREATMENT for small ($F_{(4,84)} = 2.74$; $p = 0.034$), but not for medium ($F_{(4,84)} = 1.03$; $p = 0.40$) and large spines ($F_{(4,84)} = 1.20$; $p = 0.32$), and there was a strong trend for the effect of TREATMENT in small spines ($F_{(1,21)} = 4.21$; $p = 0.053$), but no significant effect in the other groups (medium spines, $F_{(1,21)} = 1.06$, $p = 0.32$; large spines, $F_{(1,21)} < 0.0001$, $p > 0.5$). *Post hoc* testing showed that small spines of apical dendrites of CA1 pyramidal neurons increased in size at 2 h ($p = 0.036$) and 3 h ($p = 0.012$) with a trend toward spine size increases at 4 h pms ($p = 0.07$), but no significant change in spine size was detectable at 6 h pms ($p > 0.5$) compared with those in nonstimulated and otherwise equally treated control cultures. Thus, rMS showed specific effects on the structural remodeling of subpopulations of spines in our slice cultures, with rMS leading to an increase in size primarily in small spines.

Repetitive magnetic stimulation causes an increase in GluA1 cluster size and density

The above findings raised the possibility that rMS could affect the accumulation of AMPA-Rs at excitatory synapses since synaptic strength depends, at least in part, on the AMPA-R content of excitatory postsynapses, which in turn is closely linked to spine size (Matsuzaki et al., 2001). Thus, slice cultures were fixed at 3 h pms and stained for the AMPA-R subunit GluA1. Indeed, optical density measurements revealed a significant increase in GluA1 immunofluorescence in stimulated compared with nonstimulated and otherwise equally treated control cultures (Fig. 4*A*; stratum radiatum; $p = 0.028$).

In an attempt to correlate the rMS effects on GluA1 immunofluorescence with the mEPSC and spine morphology results, a different set of cultures was fixed at 1, 2, 3, 4, and 6 h pms, stained for GluA1, and the sizes and numbers of individual GluA1 clusters were assessed at high resolution (Fig. 4*B*,*C*). This analysis revealed a significant increase in both GluA1 cluster sizes ($F_{(5,36)} = 5.65$; $p < 0.001$) and numbers ($F_{(5,36)} = 11.00$; $p < 0.0001$) following rMS compared with nonstimulated and otherwise equally treated control cultures. An increase in mean GluA1 cluster sizes was detected between 2 and 4 h pms with a maximum increase of ~40% at 3 h pms (Fig. 4*C*). Moreover, the mean GluA1 cluster number was significantly increased at all time points ≥2 h after rMS (Fig. 4*C*). Notably, the percentage of apposition of GluA1 clusters with coimmunostained presynaptic synaptophysin clusters did not change following rMS (control: $82.3 \pm 2.9\%$; $83.5 \pm 2.5\%$ at 1 h pms; $86.8 \pm 2.1\%$ at 3 h pms; $82.5 \pm 2.4\%$ at 6 h pms; $n = 5$–8 cultures per group; $p = 0.71$). These data showed that rMS leads not only to a higher content of GluA1 subunits at postsynaptic sites but also to a higher number of detectable sites of GluA1 accumulation. We concluded that rMS exerts its effects on excitatory synaptic transmission by interfering with the molecular machinery that controls the accumulation of AMPA-Rs at excitatory postsynapses.

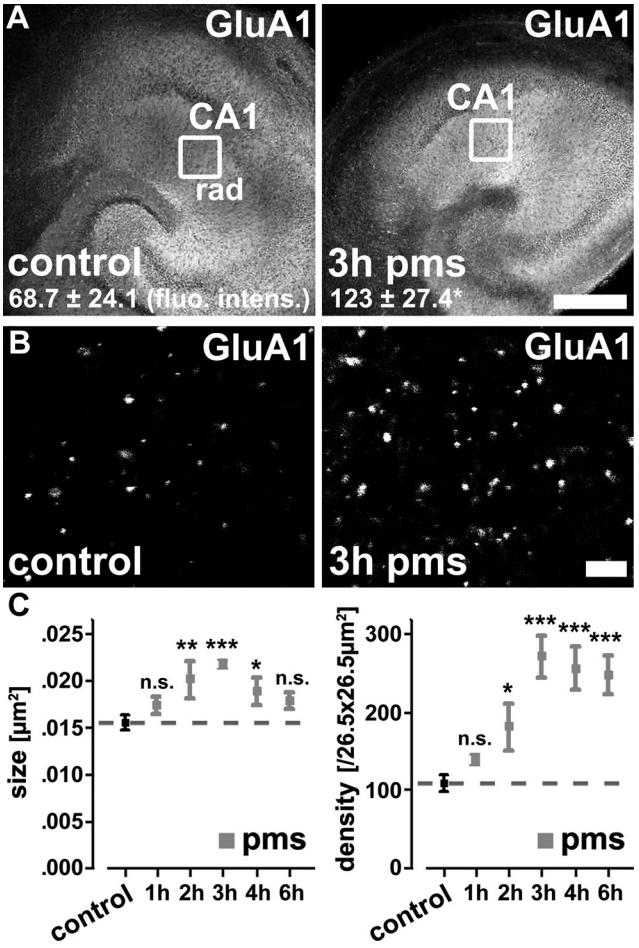

Figure 4. Repetitive magnetic stimulation *in vitro* induces changes in AMPA-R content. ***A***, Samples of nonstimulated age- and time-matched control (left) and stimulated (right) slice cultures fixed at 3 h pms stained for the AMPA-R subunit GluA1 ($n = 7$). Scale bar, 150 μm. ***B***, Samples of GluA1 clusters of control (left) and stimulated (right) slice cultures at higher magnification. Scale bar, 2 μm. ***C***, Quantification of GluA1 cluster size and density in control (pooled data from age- and time-matched nonstimulated cultures indicated by dashed line) and stimulated cultures at 1, 2, 3, 4, and 6 h pms ($n = 5$–9 cultures per group). Following rMS, a significant increase in GluA1 cluster sizes and densities was observed.

NMDA receptor-mediated synaptic neurotransmission is not changed following repetitive magnetic stimulation

To test for the specificity of the rMS effects on AMPA-R-mediated synaptic transmission, NMDA-R-mediated mEPSCs were recorded next (Fig. 5*A*,*B*). Whole-cell voltage-clamp recordings were performed at a holding potential of +40 mV in extracellular solutions containing TTX (0.5 μM), SR-95531 (10 μM), and CNQX (10 μM). Under these conditions AMPA-R-mediated inward currents (recorded at a holding potential of −70 mV; Fig. 2*A*) were completely blocked (Fig. 5*A*). Accordingly, at a holding potential of +40 mV, we were able to selectively assess NMDA-R-mediated outward currents (not containing an AMPA-R component), which could be blocked by the NMDA-R antagonist D-APV (10 μM; Fig. 5*A*). As shown in Figure 5*B*, in these experiments no significant difference in mEPSC amplitude and frequency could be detected between stimulated and nonstimulated cultures. We, therefore, concluded that NMDA-R-mediated mEPSCs are not affected by rMS at 2–4 h pms, consistent with the view that rMS induces LTP of AMPA-R-mediated excitatory synaptic transmission.

Paired recordings of CA1 pyramidal neurons

To provide further evidence for rMS-induced changes in excitatory synaptic transmission, neighboring CA1 pyramidal neurons from stimulated (at 2–4 h pms) and nonstimulated control cultures were patched simultaneously and the functional connectivity between neurons was probed (Fig. 5*C*). Up to 50 action potentials were induced at 0.1 Hz in a CA1 pyramidal neuron while recording from another. We considered a pair of neurons to be connected if >5% of presynaptic action potentials evoked time-locked current responses in the postsynaptic neuron (recorded at a holding potential of −70 mV; Fig. 5*D*). In agreement with previous work in rat hippocampal slice cultures (Debanne et al., 1995), the overall probability to find connected CA1 pyramidal neurons in nonstimulated control cultures was ~15–20%. Following rMS, a marked increase in the probability to find connected CA1 pyramidal neurons was observed (~1.5- to 2-fold; Fig. 5*E*). The mean amplitude of successfully evoked AMPA-R-mediated EPSCs in response to single presynaptic action potentials was significantly increased following rMS (Fig. 5*D*,*F*), thus supporting our findings on rMS-induced changes in AMPA-R mEPSCs (Fig. 2*C*) and GluA1 clusters (Fig. 4*C*). Interestingly, a marked decrease in the transmission failure rate was seen after rMS, that is, the percentage of action potentials not successfully evoking postsynaptic current responses in connected neurons (Fig. 5*G*). This result is consistent with an increase in the total number of functional synapses between CA1 neurons and/or changes in the presynaptic release probability (Mitra et al., 2012). Together, this set of experiments revealed that rMS leads to a more efficient and stronger excitatory synaptic coupling of CA1 pyramidal neurons in mature entorhino-hippocampal slice cultures.

NMDA receptor activation is an important step in the induction of synaptic plasticity by repetitive magnetic stimulation

The activation of ionotropic glutamate receptors of the NMDA-R subtype is known to play a crucial role in classical LTP-experiments (i.e., electrically induced LTP) (Bliss and Collingridge, 1993). Thus, we wondered whether NMDA-R activation also mediates the "LTP-like" phenomena observed in our experiments. In particular, we were interested in testing whether NMDA-Rs control the postsynaptic changes seen in CA1 pyramidal neurons after rMS. To test for this possibility, slice cultures were stimulated during pharmacological blockade of NMDA-Rs by D-APV (50 μM) and returned back to the incubator after washout of the drug. Indeed, 2–4 h after stimulation in the presence of D-APV, the rMS-induced increase in mEPSC amplitudes was abolished (Fig. 6*A*). However, an increase in mEPSC frequency was still detectable, although with a trend toward lower mEPSC frequencies compared with stimulated, but not D-APV-treated cultures (Fig. 6*A*; $p = 0.11$).

Comparable results were obtained when changes in spine sizes and GluA1 clusters were assessed (Fig. 6*B*–*D*). Pharmacological NMDA-R blockade during rMS abolished the increase in spine size (Fig. 6*B*) as well as the increases in mean GluA1 cluster size and density at 3 h pms (Fig. 6*C*,*D*). We concluded that NMDA-R activation is an important step in rMS-induced functional and structural plasticity of excitatory postsynapses in hippocampal CA1 pyramidal neurons of entorhino-hippocampal slice cultures.

Discussion

In the present study, we investigated the effects of rMS on cultured hippocampal CA1 pyramidal neurons in an organotypic environment. We report that (1) rMS induces a long-lasting in-

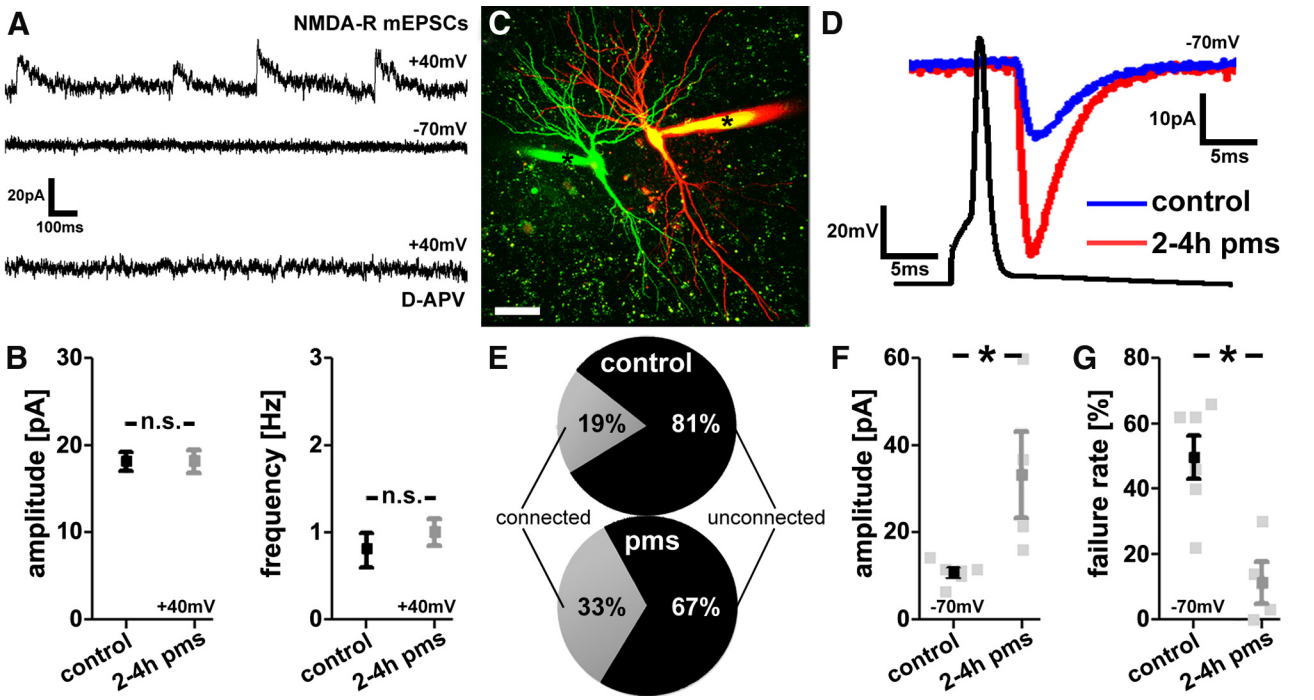

Figure 5. NMDA-R mEPSCs and paired recordings of CA1 pyramidal neurons following repetitive magnetic stimulation *in vitro*. ***A***, Sample traces of NMDA-R-mediated mEPSCs recorded at +40 mV in TTX (0.5 μM), SR-95531 (10 μM), and CNQX (10 μM). While no inward currents could be observed at −70 mV in these experiments, the outward currents recorded at +40 mV could be blocked by the NMDA-R antagonist D-APV (10 μM). ***B***, After rMS (at 2–4 h pms), neither amplitudes nor frequencies of NMDA-R-mediated mEPSCs were changed ($n = 8–10$ neurons per group; 4–5 cultures each). ***C***, Two-dimensionally projected confocal image stack of two simultaneously patched neighboring CA1 pyramidal neurons. Dye-filled patch pipettes are indicated by asterisks (Alexa 488, green; Alexa 568, red). Scale bar, 30 μm. ***D***, Averaged responses of successfully evoked time-locked postsynaptic currents recorded at −70 mV from a control (blue trace) and a stimulated CA1 pyramidal neuron (red trace). Up to 50 action potentials were induced at 0.1 Hz in the presynaptic neuron while recording from the postsynaptic CA1 neuron. ***E–G***, An increase in the percentage of connected pairs and evoked AMPA-R-mediated EPSC amplitudes was observed, while the percentage of transmission failure rate was markedly decreased after rMS (2–4 h pms; $n = 4–6$ connected pairs; 48 ± 2 action potentials probed; in 6–9 cultures; 43 connections probed total).

crease in AMPA-R-mediated excitatory synaptic strength, which (2) is accompanied by structural plasticity at the level of individual dendritic spines. Specifically, rMS leads to an enlargement of small spines. (3) These changes depend, at least in part, on the accumulation of GluA1-containing AMPA-Rs, which (4) require the activation of NMDA-Rs during rMS. These findings provide for the first time direct evidence at the cellular level that rMS induces coordinated structural and functional plasticity of excitatory postsynapses, consistent with a long-term potentiation of excitatory synaptic transmission.

Organotypic slice cultures as a model system to study cellular effects of rMS

During the past years, rTMS has received increasing interest as a noninvasive and painless brain stimulation technique to interfere with and modulate neuronal excitability (Hallett, 2007). rTMS can increase cortical excitability for hours beyond the stimulation period in humans (Ziemann et al., 2008) and has been suggested to have beneficial effects in the context of neurological diseases (Ridding and Rothwell, 2007; Edwards et al., 2008; Dimyan and Cohen, 2010; Wang et al., 2012). However, since these studies are performed at the systems level in human subjects, the cellular mechanisms underlying rTMS-induced plasticity remain unclear. Therefore, one of the major aims of the present study was to establish an *in vitro* model in which the effects of rMS on neuronal plasticity could be studied at the level of identified single neurons. To this end, we used magnetic stimulation of mouse organotypic entorhino-hippocampal slice cultures (Fig. 1*A*,*B*) and studied its effects on functional and structural properties of the CA1 synapse in stratum radiatum. This approach provides a set of noteworthy advantages as follows: The first advantage concerns standardization and reproducibility. rMS can be performed in a highly reproducible manner, with important stimulation parameters being standardized (e.g., coil distance to stimulated tissue, orientation of the stimulated tissue within the magnetic field). The second advantage concerns cellular organization and connectivity pattern. Compared with dissociated neuronal cultures, organotypic slice cultures show an excellent preservation of *in vivo* connectivity (Frotscher et al., 1995; Gähwiler et al., 1997; Holopainen, 2005). This makes it possible to perform *in vitro* experiments close to *in situ* conditions. The entorhino-hippocampal slice culture has the additional benefit of a highly laminar fiber architecture and cytoarchitecture (Förster et al., 2006). Thus, the orientation of the main fiber tracts within the magnetic field can be controlled. The third advantage concerns experimental accessibility. Neurons in cultures are readily accessible for electrophysiological recordings in combination with long-term time-lapse imaging as well as other experimental techniques. Moreover, cultured neurons can be easily influenced using, for example, pharmacological approaches. The fourth advantage concerns stimulation of intact and stable networks. In organotypic slice cultures, the effects of rMS on an *in vitro* network can be assessed in the absence of additional experimental manipulation before recordings, such as slicing of brain tissue or application of anesthetics. This is an important aspect since recent work has indicated that anesthesia has an impact on rTMS-induced plasticity (Gersner et al., 2011). Likewise, experimental evidence has accumulated that denervation, which will inevitable accompany the acute slicing of intact brains, can affect functional and structural properties of neurons (Kirov et al., 1999; McKinney et

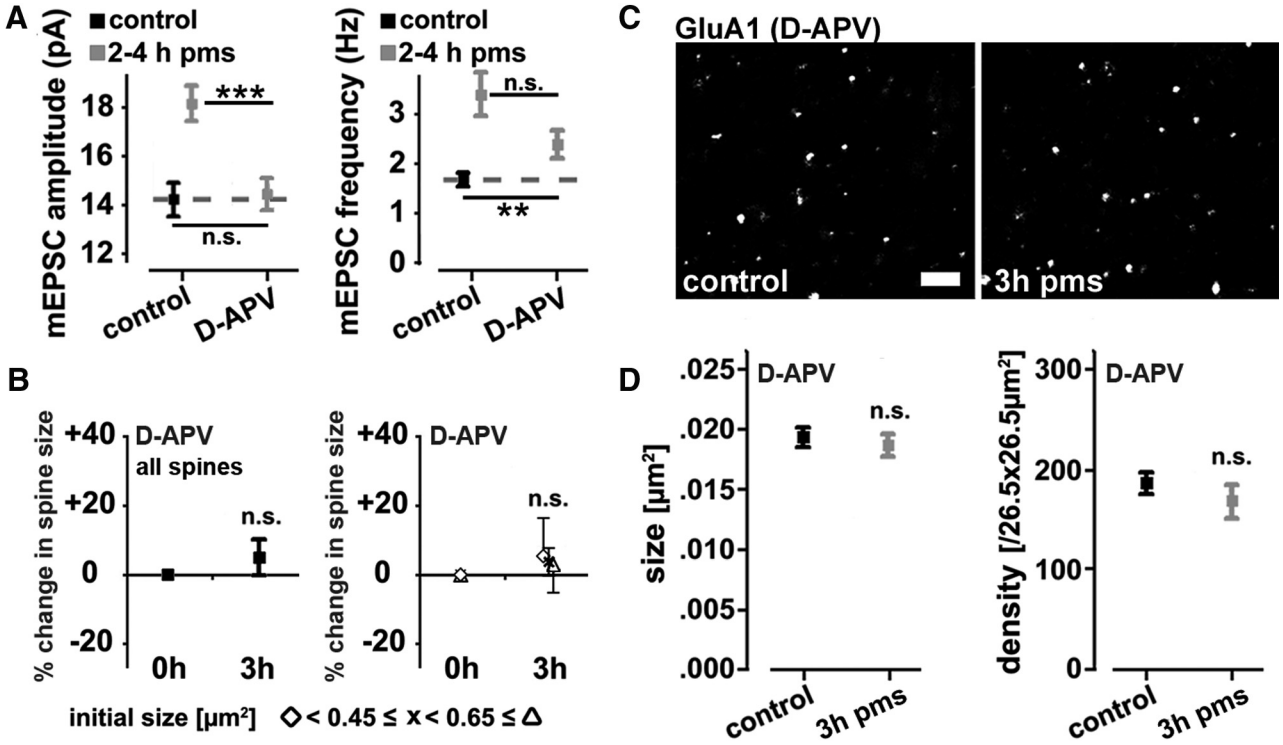

Figure 6. NMDA-R activation is required for induction of synaptic plasticity by repetitive magnetic stimulation *in vitro*. ***A***, Group data of mEPSC amplitudes and frequencies ($n = 16–27$ neurons per group; up to 5 neurons per culture; 5–11 cultures per group; age- and time-matched control data pooled with control data from Fig. 2). Stimulation of entorhino-hippocampal slice cultures in the presence of the NMDA-R inhibitor D-APV (50 μM) blocks rMS-induced changes in mEPSC amplitudes. Changes in mEPSC frequencies were not completely blocked. ***B***, The rMS-induced increase in spine size [maximum cross-sectional areas of individual spines identified before rMS (i.e., at 0 h); compare Fig. 3*C*,*E*] is not observed in cultures stimulated in the presence of D-APV (50 μM; $n = 16$ control vs $n = 6$ rMS segments; from 16 control and 5 rMS-treated cultures, respectively; age- and time-matched control data pooled with control data from Fig. 3). ***C***, Examples of D-APV (50 μM)-treated control and stimulated slice cultures stained for the AMPA-R subunit GluA1. Scale bar, 2 μm. ***D***, Quantification of GluA1 cluster size (left) and density (right) in D-APV-treated cultures ($n = 8–9$ cultures each). Stimulation in the presence of D-APV abolished the increase in GluA1 cluster size and density at 3 h pms (compare Fig. 4*B*,*C*).

al., 1999; Dinocourt et al., 2011; Vlachos et al., 2012a,b) (for review, see Steward, 1994; Deller and Frotscher, 1997). The fifth advantage concerns transgenic mouse lines. Mouse mutants (e.g., mice lacking candidate regulatory genes) can be used to study the molecular mechanisms of rMS-induced plasticity. The sixth advantage concerns knowledge transfer. The CA1 synapse in stratum radiatum is one of the best characterized synapses with respect to synaptic plasticity. Thus, data on rMS-induced synaptic plasticity can be compared with a wealth of *in vitro* and *in vivo* data obtained at this synapse under other conditions of synaptic strengthening (e.g., classical LTP paradigms). This will facilitate the identification of molecular mechanisms underlying rMS-induced plasticity. Together, we are confident that organotypic slice culture preparations, and in particular entorhino-hippocampal slice cultures, represent a suitable and potentially highly useful complementary approach to the already established experimental models to study the effects and mechanisms of rMS-induced neural plasticity.

Repetitive magnetic stimulation induces LTP of excitatory synaptic strength

Using this *in vitro* model, we found that a single high-frequency (10 Hz) magnetic stimulation protocol, which has long-lasting facilitatory aftereffects on human cortical excitability (for review, see Ziemann et al., 2008; Thut and Pascual-Leone, 2010), increased excitatory (i.e., AMPA-R-mediated) synaptic transmission in hippocampal CA1 pyramidal neurons. These changes seem to depend, at least in part, on the accumulation of the AMPA-R subunit GluA1 at synaptic sites (Bredt and Nicoll, 2003). Moreover, we provide experimental evidence that NMDA-R activation is necessary for rMS-induced synaptic plasticity [i.e., for rMS-induced changes in mEPSC amplitudes, spine sizes, and GluA1 cluster size/density (between 2 and 4 h pms)]. Of note, NMDA-R mEPSCs were not changed after rMS *in vitro*. These results are consistent with LTP of AMPA-R-mediated excitatory synaptic strength as seen in classical LTP experiments using electrical high-frequency stimulation of Schaffer collaterals (Collingridge et al., 1983; Harris et al., 1984). Although these results do not prove that increased human cortical excitability after high-frequency rTMS is due to LTP (Thickbroom, 2007), our data clearly show that repetitive magnetic stimulation is capable of inducing a long-lasting increase in excitatory synaptic strength at the single-cell level.

Repetitive magnetic stimulation induces distinct structural remodeling in subpopulations of dendritic spines

An intriguing finding of our study was the observation that rMS induces structural plasticity in distinct subpopulations of spines. In particular, small spines were found to increase their size after rMS. Small dendritic spines are highly dynamic structures (Matsuzaki et al., 2004), which express only very few AMPA-Rs (Takumi et al., 1999b; Matsuzaki et al., 2001). Notably, they can correspond to postsynaptic structures called "silent synapses" (i.e., spine synapses containing NMDA-Rs but being devoid of AMPA-Rs) (Isaac et al., 1995; Liao et al., 1995; Kerchner and Nicoll, 2008). It is interesting to speculate that spines lacking AMPA-Rs inserted GluA1 subunit-containing AMPA-Rs following rMS. This suggestion is supported by the observation that (1) the number of GluA1 clusters increased in the absence of a cor-

responding increase in spine density; (2) the percentage of synaptophysin-apposed GluA1 clusters did not change following rMS, thus rendering the extrasynaptic accumulation of GluA1 clusters unlikely; (3) AMPA-R-mediated mEPSC frequencies increased while NMDA-R-mediated mEPSCs were not altered after rMS; and (4) the probability to find connected pairs of CA1 pyramidal neurons was increased following rMS. Thus, rMS may lead to an activation of silent synapses, conveying to neurons the ability to establish new functional synaptic connections by accumulating AMPA-Rs at preexisting synapses, without the need to recruit the complete molecular machinery to form new spines and/or synapses. Regardless of these considerations, our results provide the first experimental evidence that rMS is capable of inducing structural remodeling of dendritic spines.

Presynaptic plasticity following repetitive magnetic stimulation

Since we focused on postsynaptic functional and structural plasticity in our study, rMS-induced presynaptic changes cannot be excluded at present. Although we did not observe an increase in NMDA-R-mediated mEPSCs following rMS, pharmacological inhibition of NMDA-Rs during rMS only attenuated but did not block the increase in AMPA-R-mediated mEPSC frequencies, while mEPSC amplitudes, spine sizes, and GluA1 cluster size and density remained at control levels. It thus remains to be shown whether presynaptic changes accompany the rMS-induced postsynaptic plasticity observed in our experiments and how these putative changes are regulated at the cellular/molecular level. We expect that the rMS *in vitro* model introduced in the present study will be a helpful tool to address these and other important questions in the future.

References

Ahmed Z, Wieraszko A (2006) Modulation of learning and hippocampal, neuronal plasticity by repetitive transcranial magnetic stimulation (rTMS). Bioelectromagnetics 27:288–294. CrossRef Medline

Bas Orth C, Vlachos A, Del Turco D, Burbach GJ, Haas CA, Mundel P, Feng G, Frotscher M, Deller T (2005) Lamina-specific distribution of synaptopodin, an actin-associated molecule essential for the spine apparatus, in identified principal cell dendrites of the mouse hippocampus. J Comp Neurol 487:227–239. CrossRef Medline

Benali A, Trippe J, Weiler E, Mix A, Petrasch-Parwez E, Girzalsky W, Eysel UT, Erdmann R, Funke K (2011) Theta-burst transcranial magnetic stimulation alters cortical inhibition. J Neurosci 31:1193–1203. CrossRef Medline

Bliss TV, Collingridge GL (1993) A synaptic model of memory: long-term potentiation in the hippocampus. Nature 361:31–39. CrossRef Medline

Bredt DS, Nicoll RA (2003) AMPA receptor trafficking at excitatory synapses. Neuron 40:361–379. CrossRef Medline

Capani F, Martone ME, Deerinck TJ, Ellisman MH (2001) Selective localization of high concentrations of F-actin in subpopulations of dendritic spines in rat central nervous system: a three-dimensional electron microscopic study. J Comp Neurol 435:156–170. CrossRef Medline

Collingridge GL, Kehl SJ, McLennan H (1983) Excitatory amino acids in synaptic transmission in the Schaffer collateral-commissural pathway of the rat hippocampus. J Physiol 334:33–46. Medline

Debanne D, Guérineau NC, Gähwiler BH, Thompson SM (1995) Physiology and pharmacology of unitary synaptic connections between pairs of cells in areas CA3 and CA1 of rat hippocampal slice cultures. J Neurophysiol 73:1282–1294. Medline

Deller T, Frotscher M (1997) Lesion-induced plasticity of central neurons: sprouting of single fibres in the rat hippocampus after unilateral entorhinal cortex lesion. Prog Neurobiol 53:687–727. CrossRef Medline

Dimyan MA, Cohen LG (2010) Contribution of transcranial magnetic stimulation to the understanding of functional recovery mechanisms after stroke. Neurorehabil Neural Repair 24:125–135. CrossRef Medline

Dinocourt C, Aungst S, Yang K, Thompson SM (2011) Homeostatic increase in excitability in area CA1 after Schaffer collateral transection in vivo. Epilepsia 52:1656–1665. CrossRef Medline

Edwards MJ, Talelli P, Rothwell JC (2008) Clinical applications of transcranial magnetic stimulation in patients with movement disorders. Lancet Neurol 7:827–840. CrossRef Medline

Engert F, Bonhoeffer T (1999) Dendritic spine changes associated with hippocampal long-term synaptic plasticity. Nature 399:66–70. CrossRef Medline

Feng G, Mellor RH, Bernstein M, Keller-Peck C, Nguyen QT, Wallace M, Nerbonne JM, Lichtman JW, Sanes JR (2000) Imaging neuronal subsets in transgenic mice expressing multiple spectral variants of GFP. Neuron 28:41–51. CrossRef Medline

Förster E, Zhao S, Frotscher M (2006) Laminating the hippocampus. Nat Rev Neurosci 7:259–267. CrossRef Medline

Frotscher M, Zafirov S, Heimrich B (1995) Development of identified neuronal types and of specific synaptic connections in slice cultures of rat hippocampus. Prog Neurobiol 45:143–164. CrossRef Medline

Fukazawa Y, Saitoh Y, Ozawa F, Ohta Y, Mizuno K, Inokuchi K (2003) Hippocampal LTP is accompanied by enhanced F-actin content within the dendritic spine that is essential for late LTP maintenance in vivo. Neuron 38:447–460. CrossRef Medline

Gähwiler BH, Capogna M, Debanne D, McKinney RA, Thompson SM (1997) Organotypic slice cultures: a technique has come of age. Trends Neurosci 20:471–477. CrossRef Medline

Gersner R, Kravetz E, Feil J, Pell G, Zangen A (2011) Long-term effects of repetitive transcranial magnetic stimulation on markers for neuroplasticity: differential outcomes in anesthetized and awake animals. J Neurosci 31:7521–7526. CrossRef Medline

Hallett M (2007) Transcranial magnetic stimulation: a primer. Neuron 55:187–199. CrossRef Medline

Harris EW, Ganong AH, Cotman CW (1984) Long-term potentiation in the hippocampus involves activation of *N*-methyl-D-aspartate receptors. Brain Res 323:132–137. CrossRef Medline

Harris KM, Jensen FE, Tsao B (1992) Three-dimensional structure of dendritic spines and synapses in rat hippocampus (CA1) at postnatal day 15 and adult ages: implications for the maturation of synaptic physiology and long-term potentiation. J Neurosci 12:2685–2705. Medline

Harvey CD, Svoboda K (2007) Locally dynamic synaptic learning rules in pyramidal neuron dendrites. Nature 450:1195–1200. CrossRef Medline

Hellmann J, Jüttner R, Roth C, Bajbouj M, Kirste I, Heuser I, Gertz K, Endres M, Kronenberg G (2012) Repetitive magnetic stimulation of human-derived neuron-like cells activates cAMP-CREB pathway. Eur Arch Psychiatry Clin Neurosci 262:87–91. CrossRef Medline

Holbro N, Grunditz A, Oertner TG (2009) Differential distribution of endoplasmic reticulum controls metabotropic signaling and plasticity at hippocampal synapses. Proc Natl Acad Sci U S A 106:15055–15060. CrossRef Medline

Holopainen IE (2005) Organotypic hippocampal slice cultures: a model system to study basic cellular and molecular mechanisms of neuronal cell death, neuroprotection, and synaptic plasticity. Neurochem Res 30:1521–1528. CrossRef Medline

Isaac JT, Nicoll RA, Malenka RC (1995) Evidence for silent synapses: implications for the expression of LTP. Neuron 15:427–434. CrossRef Medline

Jourdain P, Fukunaga K, Muller D (2003) Calcium/calmodulin-dependent protein kinase II contributes to activity-dependent filopodia growth and spine formation. J Neurosci 23:10645–10649. Medline

Keck ME, Welt T, Post A, Müller MB, Toschi N, Wigger A, Landgraf R, Holsboer F, Engelmann M (2001) Neuroendocrine and behavioral effects of repetitive transcranial magnetic stimulation in a psychopathological animal model are suggestive of antidepressant-like effects. Neuropsychopharmacology 24:337–349. CrossRef Medline

Kerchner GA, Nicoll RA (2008) Silent synapses and the emergence of a postsynaptic mechanism for LTP. Nat Rev Neurosci 9:813–825. CrossRef Medline

Kirov SA, Sorra KE, Harris KM (1999) Slices have more synapses than perfusion-fixed hippocampus from both young and mature rats. J Neurosci 19:2876–2886. Medline

Levkovitz Y, Marx J, Grisaru N, Segal M (1999) Long-term effects of transcranial magnetic stimulation on hippocampal reactivity to afferent stimulation. J Neurosci 19:3198–3203. Medline

Liao D, Hessler NA, Malinow R (1995) Activation of postsynaptically silent

synapses during pairing-induced LTP in CA1 region of hippocampal slice. Nature 375:400–404. CrossRef Medline

Lisman JE (2009) The pre/post LTP debate. Neuron 63:281–284. CrossRef Medline

Maletic-Savatic M, Malinow R, Svoboda K (1999) Rapid dendritic morphogenesis in CA1 hippocampal dendrites induced by synaptic activity. Science 283:1923–1927. CrossRef Medline

Matsuzaki M, Ellis-Davies GC, Nemoto T, Miyashita Y, Iino M, Kasai H (2001) Dendritic spine geometry is critical for AMPA receptor expression in hippocampal CA1 pyramidal neurons. Nat Neurosci 4:1086–1092. CrossRef Medline

Matsuzaki M, Honkura N, Ellis-Davies GC, Kasai H (2004) Structural basis of long-term potentiation in single dendritic spines. Nature 429:761–766. CrossRef Medline

McKinney RA, Capogna M, Dürr R, Gähwiler BH, Thompson SM (1999) Miniature synaptic events maintain dendritic spines via AMPA receptor activation. Nat Neurosci 2:44–49. CrossRef Medline

Mitra A, Mitra SS, Tsien RW (2012) Heterogeneous reallocation of presynaptic efficacy in recurrent excitatory circuits adapting to inactivity. Nat Neurosci 15:250–257. CrossRef Medline

Moliadze V, Zhao Y, Eysel U, Funke K (2003) Effect of transcranial magnetic stimulation on single-unit activity in the cat primary visual cortex. J Physiol 553:665–679. CrossRef Medline

Nägerl UV, Eberhorn N, Cambridge SB, Bonhoeffer T (2004) Bidirectional activity-dependent morphological plasticity in hippocampal neurons. Neuron 44:759–767. CrossRef Medline

Ridding MC, Rothwell JC (2007) Is there a future for therapeutic use of transcranial magnetic stimulation? Nat Rev Neurosci 8:559–567. CrossRef Medline

Salinas FS, Szabó CÁ, Zhang W, Jones L, Leland MM, Wey HY, Duong TQ, Fox PT, Narayana S (2011) Functional neuroimaging of the baboon during concurrent image-guided transcranial magnetic stimulation. Neuroimage 57:1393–1401. CrossRef Medline

Segal M, Greenberger V, Korkotian E (2003) Formation of dendritic spines in cultured striatal neurons depends on excitatory afferent activity. Eur J Neurosci 17:2573–2585. CrossRef Medline

Siebner HR, Bergmann TO, Bestmann S, Massimini M, Johansen-Berg H, Mochizuki H, Bohning DE, Boorman ED, Groppa S, Miniussi C, Pascual-Leone A, Huber R, Taylor PC, Ilmoniemi RJ, De Gennaro L, Strafella AP, Kähkönen S, Klöppel S, Frisoni GB, George MS, et al. (2009) Consensus paper: combining transcranial stimulation with neuroimaging. Brain Stimul 2:58–80. CrossRef Medline

Steward O (1994) Reorganization of neuronal circuitry following central nervous system trauma: naturally occurring processes and opportunities for therapeutic intervention. In: The Neurobiology of central nervous system trauma (Salzman SK, Faden AI, eds), pp 266–287. New York: Oxford UP.

Stoppini L, Buchs PA, Muller D (1991) A simple method for organotypic cultures of nervous tissue. J Neurosci Methods 37:173–182. CrossRef Medline

Takumi Y, Matsubara A, Rinvik E, Ottersen OP (1999a) The arrangement of glutamate receptors in excitatory synapses. Ann N Y Acad Sci 868:474–482. CrossRef Medline

Takumi Y, Ramírez-León V, Laake P, Rinvik E, Ottersen OP (1999b) Different modes of expression of AMPA and NMDA receptors in hippocampal synapses. Nat Neurosci 2:618–624. CrossRef Medline

Thickbroom GW (2007) Transcranial magnetic stimulation and synaptic plasticity: experimental framework and human models. Exp Brain Res 180:583–593. CrossRef Medline

Thut G, Pascual-Leone A (2010) A review of combined TMS-EEG studies to characterize lasting effects of repetitive TMS and assess their usefulness in cognitive and clinical neuroscience. Brain Topogr 22:219–232. CrossRef Medline

Trippe J, Mix A, Aydin-Abidin S, Funke K, Benali A (2009) Theta burst and conventional low-frequency rTMS differentially affect GABAergic neurotransmission in the rat cortex. Exp Brain Res 199:411–421. CrossRef Medline

Valero-Cabré A, Payne BR, Rushmore J, Lomber SG, Pascual-Leone A (2005) Impact of repetitive transcranial magnetic stimulation of the parietal cortex on metabolic brain activity: a ^{14}C-2DG tracing study in the cat. Exp Brain Res 163:1–12. CrossRef Medline

Vlachos A, Maggio N, Segal M (2008) Lack of correlation between synaptopodin expression and the ability to induce LTP in the rat dorsal and ventral hippocampus. Hippocampus 18:1–4. CrossRef Medline

Vlachos A, Korkotian E, Schonfeld E, Copanaki E, Deller T, Segal M (2009) Synaptopodin regulates plasticity of dendritic spines in hippocampal neurons. J Neurosci 29:1017–1033. CrossRef Medline

Vlachos A, Bas Orth C, Schneider G, Deller T (2012a) Time-lapse imaging of granule cells in mouse entorhino-hippocampal slice cultures reveals changes in spine stability after entorhinal denervation. J Comp Neurol 520:1891–1902. CrossRef Medline

Vlachos A, Becker D, Jedlicka P, Winkels R, Roeper J, Deller T (2012b) Entorhinal denervation induces homeostatic synaptic scaling of excitatory postsynapses of dentate granule cells in mouse organotypic slice cultures. PLoS One 7:e32883. CrossRef Medline

Wang RY, Tseng HY, Liao KK, Wang CJ, Lai KL, Yang YR (2012) rTMS combined with task-oriented training to improve symmetry of interhemispheric corticomotor excitability and gait performance after stroke: a randomized trial. Neurorehabil Neural Repair 26:222–230. CrossRef Medline

Yasumatsu N, Matsuzaki M, Miyazaki T, Noguchi J, Kasai H (2008) Principles of long-term dynamics of dendritic spines. J Neurosci 28:13592–13608. CrossRef Medline

Ziemann U, Paulus W, Nitsche MA, Pascual-Leone A, Byblow WD, Berardelli A, Siebner HR, Classen J, Cohen LG, Rothwell JC (2008) Consensus: motor cortex plasticity protocols. Brain Stimul 1:164–182. CrossRef Medline